Green Chemistry

Accepted Manuscript

ROYAL SOCIETY OF CHEMISTRY

rsc.li/green-chem

Journal Name ARTICLE

View Article Online
DOI: 10.1039/C7GC03436A

Metal-free remote-site C–H alkenylation: regio- and diastereoselective synthesis of solvatochromic dyes

Received 00th January 20xx,
Accepted 00th January 20xx

DOI: 10.1039/x0xx00000x

www.rsc.org/

María José Albaladejo,[a,†] María José González-Soria[a] and Francisco Alonso*[a]

Lately, the transition-metal catalysed C-H alkenylation of nitrogen heterocycles has gained increasing attention, often with the intervention of complex and expensive catalytic systems. On the other hand, both, chalcones and indolizines are versatile families of compounds with applications in diverse research areas, including materials science, because of their prominent photophysical attributes. We set forth herein the metal-free regio- and diastereoselective C-H alkenylation of indolizines through a very simple and mild acid-base approach. The most fascinating fact in this remote-site C_{sp2}-C_{sp2} bond formation is that only one starting material is utilised, which undergoes a formal self-alkenylation to integrate a chalcone moiety and furnish a new family of dyes; a plausible reaction mechanism has been put forward. A one-pot multicomponent protocol has been conceived that in-situ generates the starting indolizine and has been extended to a multi-gram scale synthesis with equal efficiency. The dyes show a single structure in the solid state but two stable structures in solution (rotamers). Preliminary studies on the optical properties of the dyes reveal a particle-size dependent colour in the solid state and solvatochromism (i.e., different colours in solution depending on the solvent polarity). Remarkably, the solvatochromic behaviour has also been displayed in plastics. We believe that this finding opens new avenues in the fields of heterocyclic chemistry, dyes, and materials science.

Introduction

There is a general upsurge of interest in developing more efficient and sustainable processes for the alkenylation of aromatic and heteroaromatic compounds based on C-H activation. Among them, the transition-metal free cross-coupling of aryl halides with alkenes is praiseworthy but requires the action of strong bases that curtail the substrate scope of the method.[1] The cross-dehydrogenative coupling (CDC) of arenes and alkenes (oxidative Heck-type or Fujiwara-Moritani reaction) represents a much more advantageous and resourceful strategy because skips the pre-installation of the halide on the aromatic unit and produces hydrogen as the only byproduct (i.e., high atom economy).[2] At any rate, the presence of a noble transition metal is mandatory, normally accompanied by a stoichiometric amount of an oxidant under thermal treatment; ruthenium,[3] rhodium[4] and, especially, palladium[5] catalysts dominate over other metals in this field. The control of both the regio- and stereoselectivity are major issues in this type of reactions; the former is commonly addressed by the introduction of a directing group (e.g., ortho alkenylation) or by activation of HetC_{sp2}-H bonds (e.g., NC_{sp2}-H bonds). Remote site-selective C_{sp2}-H olefination is, yet, a much more challenging and hot topic.[6]

In recent years, a great deal of attention has been devoted to the selective alkenylation of nitrogen heterocycles making use of the power of the CDC tool;[7] this additional introduction of functionality can be ultimately used for further synthetic purposes or to enhance the inherent biological activity of the compounds. Pyridines,[8] indole derivatives,[9] uracils,[10] imidazo[1,2-*a*]pyridines[11] and indolizines[12] are some of the substrates successfully subjected to this reaction (Scheme 1). However, the corresponding methods implemented are far from being green and sustainable, and conditional on close site-selective C-H activation. Furthermore, it seems rather unviable to scale up the procedures from the economic (expensive catalysts), safety (high temperatures in O_2 atmosphere) and environmental point of view (use of non-recommended solvents[13]). Therefore, there is a justification to explore new routes towards heterocycle alkenylation. Moreover, the alkenylation of aromatics by C-H activation also elongates the π system, producing conjugated organic materials with potential exploitation of their photophysical characteristics (e.g., as organic electronic materials).[14]

In relation with the latter topic, organic dyes with a D-π-A configuration contain both electron-donating (D) and electron-withdrawing groups (A) connected by a π-conjugated section; alternatively, a D-A-π-A configuration can be molecularly designed where the additional intercalated A is a heterocyclic component (Fig. 1). The particular light absorption of these compounds makes them ideal candidates for chemosensors[15] and dye-sensitised solar cells.[16] The construction of the alkenyl linker usually relies on a Wittig reaction, for which a proper functionalisation of the starting materials is required.

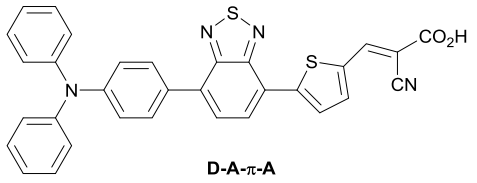

D-A-π-A

Fig. 1 Dye with a D-A-π-A configuration.

On the other hand, such different types of compounds as indolizines[17] and chalcones[18] have manifold pharmacological activities in common, namely: antioxidant, anti-tubercular, anti-inflammatory, antifungal, antibacterial, anticancer or

[a] *Instituto de Síntesis Orgánica (ISO) and Departamento de Química Orgánica, Facultad de Ciencias, Universidad de Alicante, Apdo. 99, 03080 Alicante, Spain; E-mail: falonso@ua.es*

Electronic Supplementary Information (ESI) available: [general, procedures, characterisation data, UV-Vis and NMR spectra (PDF); X-ray crystallographic data (CIF); video (MPEG4)]. See DOI: 10.1039/x0xx00000x

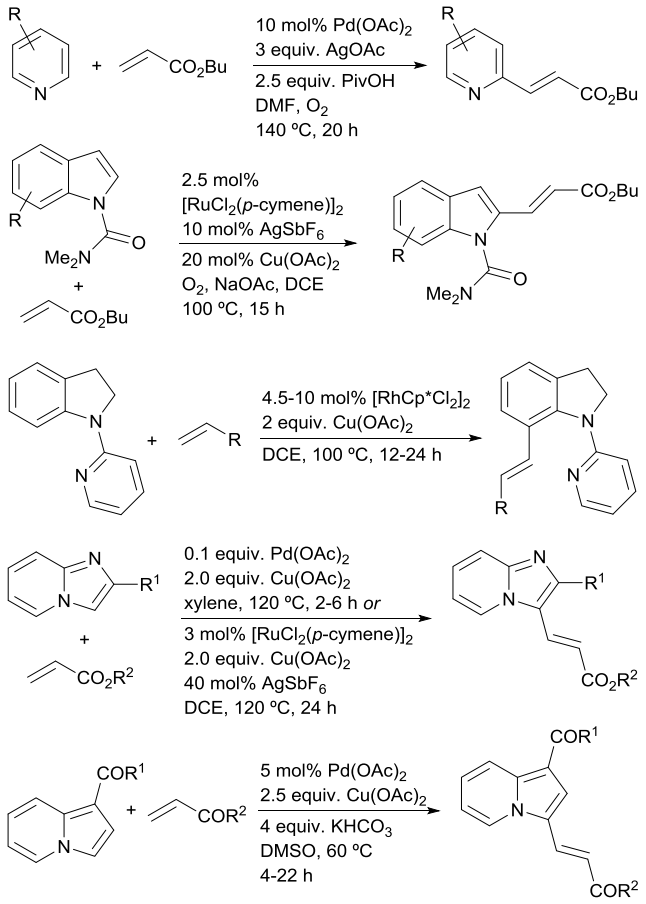

Scheme 1 Transition-metal catalysed alkenylation of some N-heterocycles.

analgesic activities. Among them, the outstanding antibacterial activity of some heterocyclic chalcones is worth of mention.[19] Moreover, both the indolizine[20] and pyridinyl chalcone[18a,21] systems are very useful scaffolds in synthetic organic chemistry as well as in materials science. In the latter respect, indolizine dyes have found practical applications as materials in laser-based recording and reading devices,[22] thermography and fotothermography,[22a] electrochromic devices,[23] optical filters,[24] as well as photoelectric converters.[25] Companies of international renown have shown considerable concern for this type of materials.[22,24,25] Within the most recent literature, several articles covering the photophysical behaviour (e.g., halochromism, fluorescence, etc.) of indolizine[26] and heterocyclic chalcone dyes[27] have been reported (Fig. 2). It is worth noting that the more specific 2-pyridinyl chalcones[27b-f] can additionally behave as probes for sensing of metal ions by coordination through the 2-pyridinylcarbonyl fragment.

As part of our dedication to study the application of supported copper nanoparticles to multicomponent reactions,[28] we reported the three-component synthesis of indolizines from pyridine-2-carbaldehyde derivatives, secondary amines and terminal alkynes catalysed by copper nanoparticles on activated carbon (CuNPs/C) in dichloromethane (Scheme 2).[29] Interestingly, heterocyclic chalcones were obtained from the same starting materials in the absence of solvent. Despite the easiness to prepare 1-amino-3-substituted indolizines, the reactivity of this class of heterocyclic compounds remains

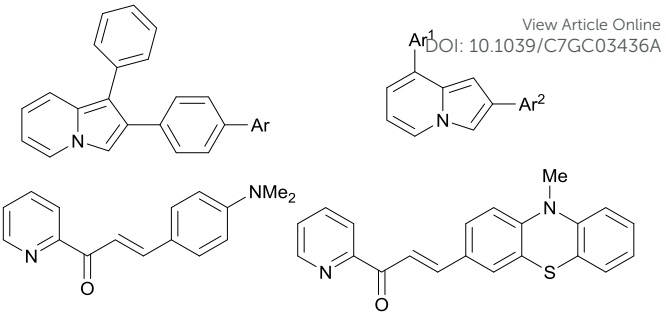

Fig. 2 Indolizines and heterocyclic chalcones with relevant photophysical properties.

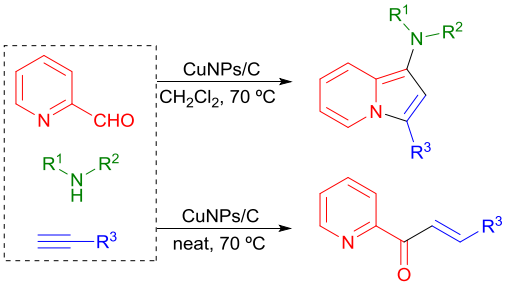

Scheme 2 Synthesis of indolizines and heterocyclic chalcones.

unexplored. Only very recently, we demonstrated that this type of indolizines could be transformed into indolizidines though a highly chemo- and diastereoselective catalytic hydrogenation.[30]

Considering the aforementioned features of indolizines and heterocyclic chalcones and concluding this introduction, we can say that it is timely to elaborate new structures and synthetic pathways for these kind of compounds. Particularly interesting is the possibility to assemble the indolizine and chalcone moieties in the same molecule through highly effective and simple alkenylation methods. We wish to present herein the discovery of a new family of dyes with a D-A-π-A configuration and a crossed indolizine-chalcone motif, which are obtained by simple acid-base treatment of the parent indolizines (Scheme 3);[31] the reaction mechanism, a structural interpretation of the dyes in the solid state and in solution, as well as some of their optical properties are also tackled.

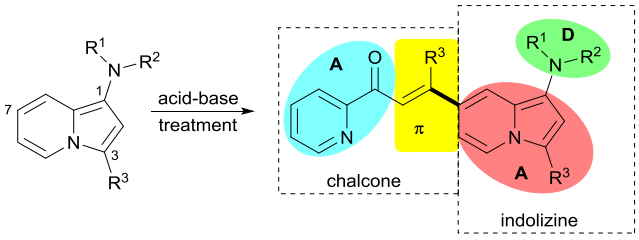

Scheme 3 General synthesis of the dyes

Results and discussion

The starting indolizines **1** were synthesized by the three-component reaction of pyridine-2-carbaldehyde derivatives, secondary amines and terminal alkynes catalysed by CuNPs/C.[29] Their response to acidic medium is first presented.

Optimisation of the reaction conditions

Indolizine **1a**, derived from pyridine-2-carbaldehyde, dibenzylamine and phenylacetylene, was deployed as the model compound in order to settle the optimum reaction conditions. A range of acids was tested at room temperature, followed by neutralisation with saturated solution of $NaHCO_3$ (Table 1): mineral acids or strong organic acids did not produce **2a** (Table 1, entries 1–3, 7 and 8). Better performance was observed for the propionic and acetic carboxylic acids; the highest conversion was attained using acetic acid either at room temperature or at 50 ºC (Table 1, entries 5 and 10), whereas dilution of acetic acid or higher temperature had a deleterious effect on the yield (Table 1, entries 9 and 11). Careful monitoring of the standard reaction with HOAc at ambient temperature brought into view a quantitative conversion of **1a** after 6 h and an isolated yield of about 70% of **2a** (Table 1, entry 12).

Table 1 Reaction of the indolizine **1a** with different acids[a]

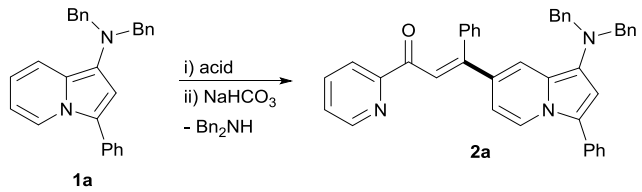

Entry	Acid	T (ºC)	*t* (h)	Yield[b] (%)
1	H_2SO_4	rt	16	-
2	H_2SO_4-MeOH[c]	rt	16	-
3	HNO_3	rt	16	-
4	HCO_2H	rt	16	10
5	HOAc	rt	16	67
6	$CH_3CH_2CO_2H$	rt	16	57
7	CF_3CO_2H	rt	6	-
8	CH_3SO_3H	rt	16	-
9	HOAc-H_2O[d]	rt	16	-
10	HOAc	50	16	69
11	HOAc	80	16	25
12	HOAc	rt	6	70

[a] Reaction conditions: **1a** (0.5 mmol), acid (3 mL); then, sat. $NaHCO_3$ until neutralisation. [b] Isolated yield of **2a** based on 2 equiv. of **1a**. [c] Three drops of the acid in 3 mL of MeOH. [d] HOAc-H_2O 1:1.

Substrate scope

In view of the above optimisation, the outreach of this transformation was studied with a minimum time of treatment with HOAc of 6 h. We first studied the effect of the substitution on the 3-aryl group for a series of 1-dibenzylamino indolizine derivatives (Table 2). The presence of electron-donating groups at the *para* position (**1b** and **1c**) was found to be somewhat beneficial with respect to the unsubstituted counterpart (**1a**), with the corresponding dyes (**2b** and **2c**) being obtained in good isolated yields. The opposite effect was noted for the existence of *para* electron-withdrawing groups, with yields around 50% for **2d** and **2e**. The substitution of the 3-aryl into a 3-alkyl substituent in **1** exerted a certain detrimental effect (compare **2f** with **2a**). Next, we explored the influence of the amino substituents: the yield also decreased when replacing a benzyl with a methyl group (compare **2g** with **2a**). The yield shrinkage was more pronounced in the case of *N*-methyl-*N*-phenethyl- (**2h**), *N*-piperidinyl- (**2i**) or *N*,*N*-dibutylamino (**2j**) substituents; the reaction was especially slow in the two latter cases. Dyes bearing a *N*-methyl-*N*-phenyl moiety could be also synthesized, either containing the normal indolizine/pyridinyl (**2k**) in good yield, or the 5-methylindolizine/6-methylpyridinyl (**2l**) nuclei in very modest yield. Pleasantly, the yield was boosted above 70% when two strong electron-donating groups (i.e., 4-methoxyphenyl) were bonded to nitrogen (**2m**). This method was proven to be effectual for the construction of chiral dyes, such in the case of the (*R*)-*N*-benzyl-*N*-(α-methyl)benzylamino derivative **2n**. It can be concluded that the existence of the 1-dibenzylamino and 3-aryl groups is, in general, essential to obtain good yields. Unfortunately, attempts to obtain the cross-alkenylated products from two different indolizines (**1a** with **1b**, **1c** and **1d**) were unfruitful due to the lack of selectivity.

In order to upgrade the effectiveness of the process, a three-component one-pot protocol was developed from pyridine-2-carbaldehyde, dibenzylamine and phenylacetylene, without a need to isolate the intermediate indolizine **1a** (Scheme 4). It was gratifying to check that the reaction outcome was very similar to that of the pre-formed indolizine.

Scale up is a hurdle generally encountered in organic synthesis, more markedly in multi-step procedures and in catalysis, which often curtails the transfer of laboratory basic research into the productive sector. In this vein, we strove to adapt the preceding one-pot method to a multi-gram scale (see the ESI for full details). For this purpose, several parameters were readjusted: (a) 0.5 mol% CuNPs/C was exchanged for 5 mol% CuI, with the latter being commercially available and readily accessible for anyone interested in manufacturing this type of dyes; (b) the reaction was made greener by removing CH_2Cl_2 and working under solvent-free conditions; (c) the neutralisation step was executed with NaOH solution instead of sat. $NaHCO_3$ to avoid excessive bubbling; and (d) the purification of the dye was accomplished by recrystallisation in lieu of column chromatography, with the former being always preferred by the chemical industry. We must underline that the use of CuNPs/C is advantageous because enables an

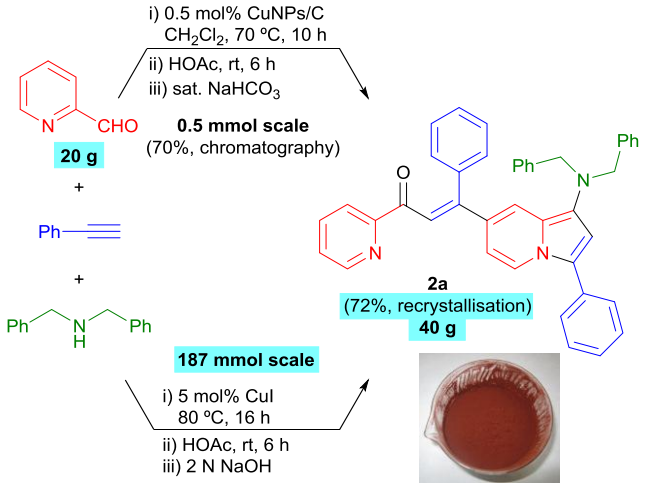

Scheme 4 One-pot synthesis of the dye **2a** at 0.5 and 187 mmol scale from commercial starting materials.

View Article Online
DOI: 10.1039/C7GC03436A

Table 2 Synthesis of the dyes **2** from the indolizines **1**[a,b]

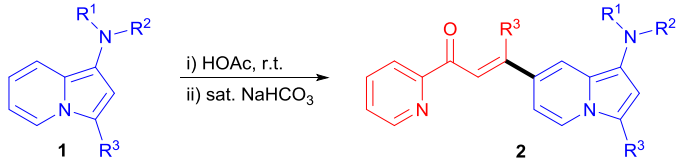

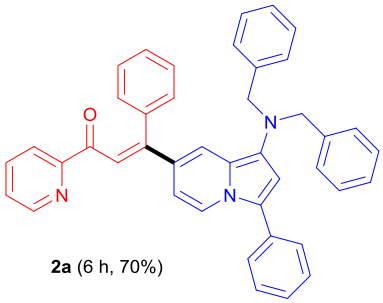

2a (6 h, 70%)

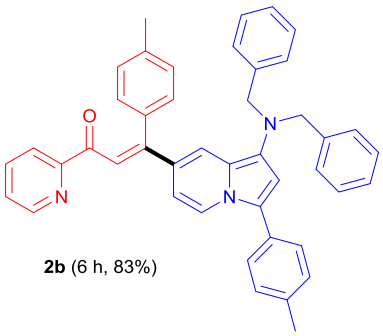

2b (6 h, 83%)

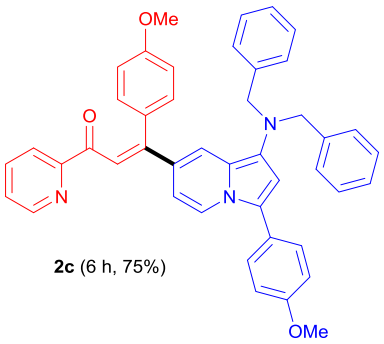

2c (6 h, 75%)

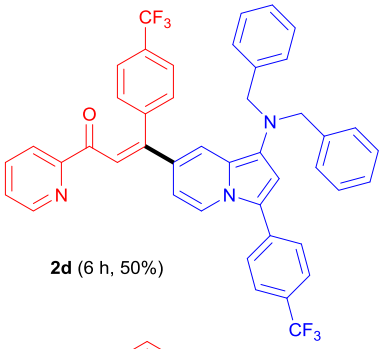

2d (6 h, 50%)

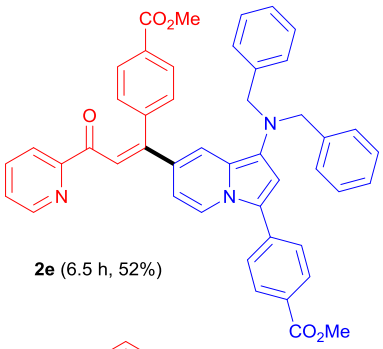

2e (6.5 h, 52%)

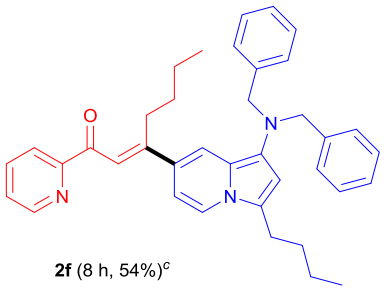

2f (8 h, 54%)[c]

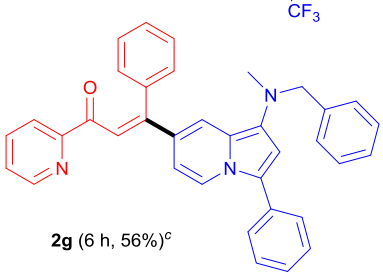

2g (6 h, 56%)[c]

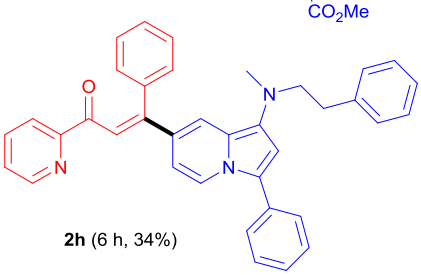

2h (6 h, 34%)

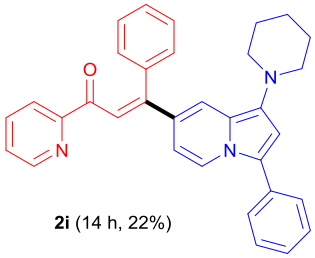

2i (14 h, 22%)

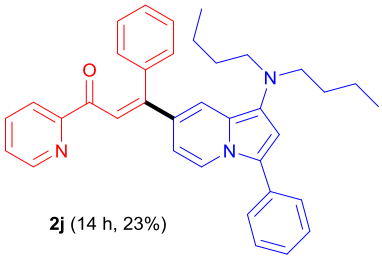

2j (14 h, 23%)

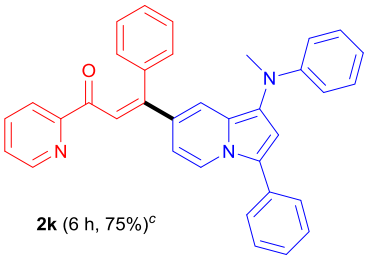

2k (6 h, 75%)[c]

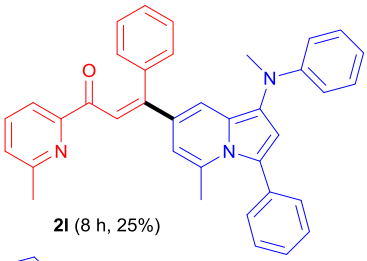

2l (8 h, 25%)

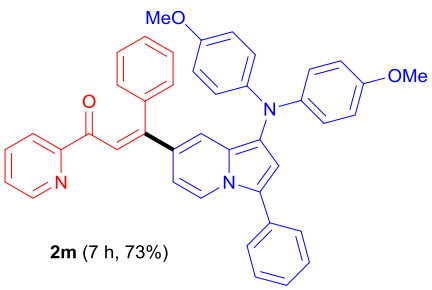

2m (7 h, 73%)

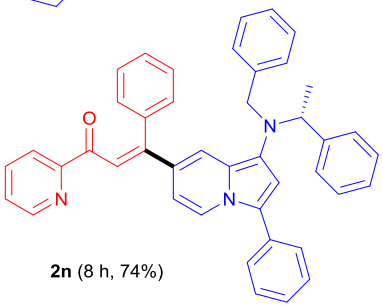

2n (8 h, 74%)

[a] Reaction conditions: indolizine **1** (0.5 mmol) and HOAc (3 mL) at rt for the specified time; then sat. $NaHCO_3$ until neutralisation. [b] Yield of the isolated product **2** based on 2 equiv. of **1**. [c] NMR yield based on 2 equiv. of **1**.

adequate metal separation from the reaction medium by filtration; in contrast, with CuI, washing with ammonia solution is suggested during the work-up for copper removal. Nevertheless, in this manner, 187 mmol (20 g) of pyridine-2-carbaldehyde were converted to 40 g of the pure dye **2a** (Scheme 4). The yield achieved (72%) is concordant with that of the small-scale synthesis and denotes a highly reproducible and robust method.

Structural analysis

From the structural viewpoint, we were delighted to find out that the resulting trisubstituted indolizine dyes **2** maintained the original structure of the starting material **1**, but had grown up through the 7-position of the indolizine nucleus by the incorporation of a heterocyclic chalcone fragment from another indolizine molecule. In this sense, the dyes **2** can be considered as indolizine-chalcone hybrids selectively bonded through a C_{sp2}-C_{sp2} bond. Certainly, this is a very singular C_{sp2}-C_{sp2} bond formation with the following salient features: (a) the conversion of **1** into **2** can be formally considered as a remote-site C–H self-alkenylation reaction; (b) transition-metal catalysis is dispensable; (c) contrary to the published alkenylation strategies which result in (quaternary)C_{sp2}-(tertiary)C_{sp2} bond formation, the more challenging (quaternary)C_{sp2}-(quaternary)C_{sp2} bonds are made now (i.e., with a 1,1-disubstituted alkenyl fragment); (d) it is worthwhile mentioning the extraordinary selectivity achieved in this reaction, with the dyes **2** being obtained with absolute control of both the regioselectivity and the stereoselectivity. Thus, out of the ten potential isomers which can be drawn as products (five possible regioisomers at the indolizine positions 2, 5, 6, 7, and 8, each as two possible *Z*/*E* diastereoisomers), only one was formed, the 7-substituted *E* isomer.

The structure of the dyes **2** was unequivocally established by X-ray crystallography of **2a** and **2c** (Fig. 3).[32] The X-ray plot of **2a** brings into view a quasi-flat arrangement of the chalcone-indolizine backbone. Conversely, the phenyl group at the β-position of the C=O (C15–C16) lays near perpendicular to that backbone (C17–C16–C15–C22 torsion angle = 80º) in order to reduce the steric interaction of the ortho Hs with the C=O and the C5–H. The phenyl ring on the indolizine heterocycle also appears deviated from co-planarity (C2–C1–C9–C14 torsion angle = 31º) to prevent C2–H/C14–H and C8–H/C10–H interactions. Finally, the carbonyl group and the C–N of the pyridinyl group are exposed to view in an anti-periplanar conformation (O1–C23–C24–N2) to minimise dipole-dipole interactions. The structural X-ray patterns displayed by the dyes **2a** and **2c** were alike.

Surprisingly, the response of the dyes in solution was very different from that in the solid state: duplicity of some NMR signals was observed for all compounds **2** except **2f**. For instance, compound **2a** exhibited a *ca.* 1:5 signal ratio in ^{1}H NMR ($CDCl_3$) which was constant irrespective of the reaction conditions or purification method (chromatography or recrystallisation). Apparently, compounds **2** exist as a mixture of two distinguishable rotamers in solution (Fig. 4); the fact that the above ratio varies with the NMR solvent used would

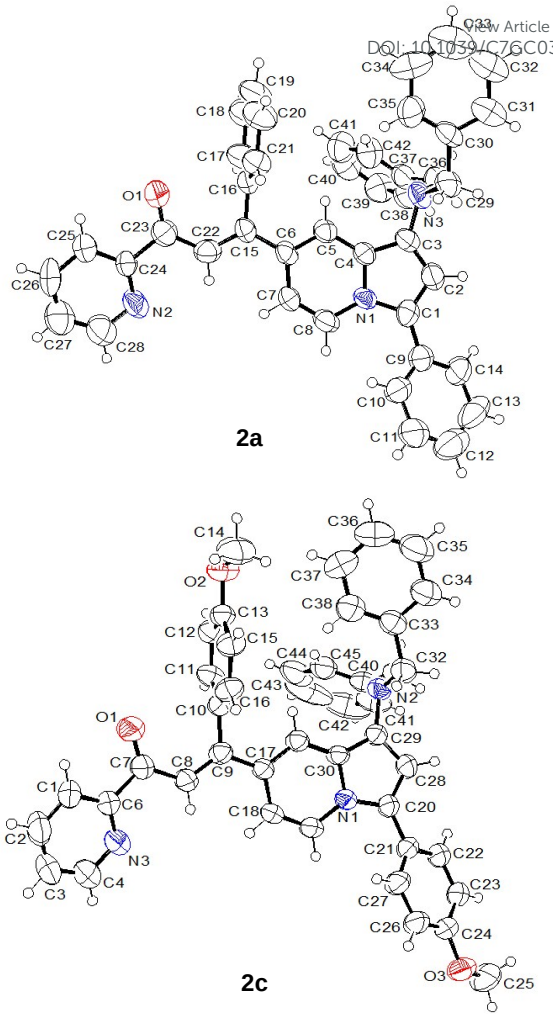

Fig. 3 Plot showing the X-ray structure and atom numbering of the dyes **2a** and **2c**.

bolster this hypothesis (Table 3). In general, the major rotamer seems to be favoured in the more polar solvents (Table 3, compare entry 2 with 5, 7 and 8); this fact entails important consequences in the optical performance of the dyes (see below). The trend to signal coalescence and to equal the population species, noticed by heating, is also typical of rotamers (Table 3, entries 5 and 6).[33]

The coexistence of the two rotamers could be ascribed to the circumstance that compounds **2** are push-pull highly conjugated systems, possessing the electron-releasing and -withdrawing amino and acyl groups, respectively. Therefore, resonant forms with a partial double bond connecting the chalcone and indolizine core could be drawn (Scheme 5a). The restricted rotation around that bond would lead to two highly conjugated and conformationally stable η-enaminoketones. NOESY experiments are in agreement with the rotamer **A** being the major one which, in turn, coincides with the structure of **2a** in the solid state (Scheme 5b). The conformation suggested for rotamer **B** is more dubious, albeit it is evident that $H_{d'}$ and $H_{k'}$ are far each other now (Scheme 5b). In fact, these two protons experienced the most pronounced variation in the chemical shift (*ca.* 0.40 and 0.55 ppm, respectively) with a displacement to a higher field

View Article Online
DOI: 10.1039/C7GC03436A

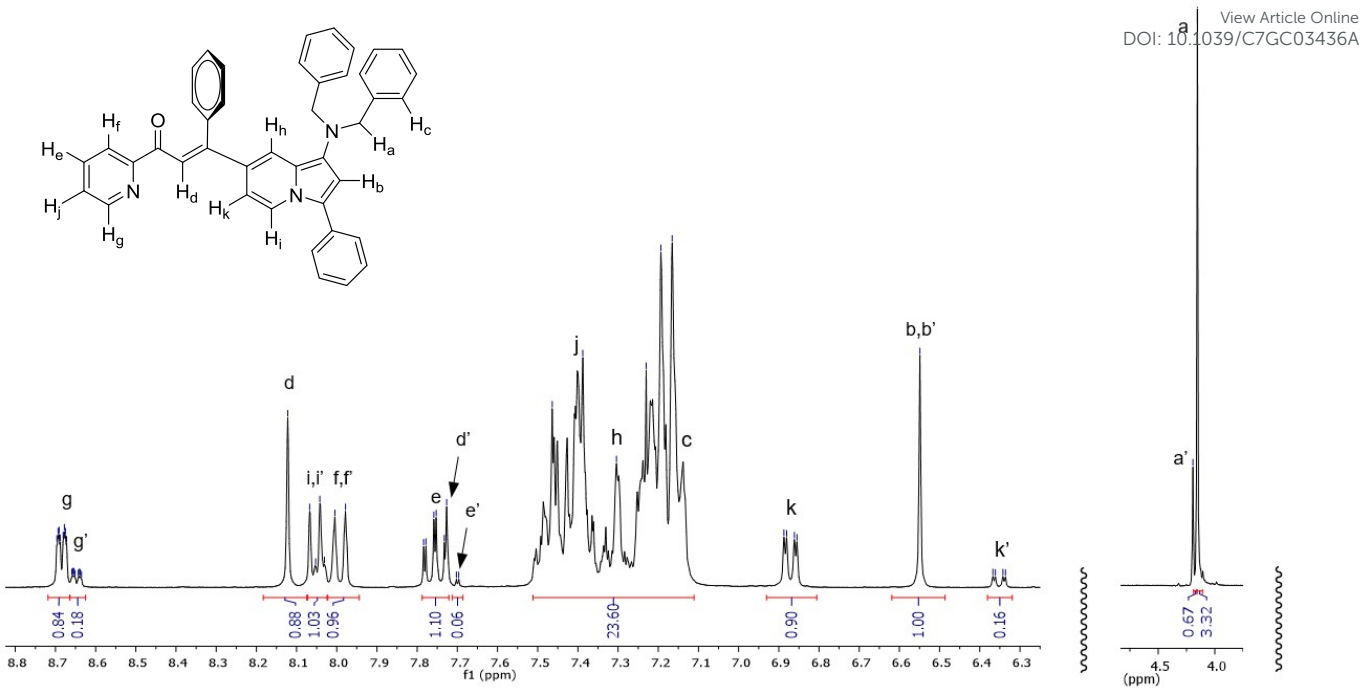

Fig. 4 Partial assignment of the ^{1}H NMR signals of **2a** ($CDCl_3$). Letters with a prime denote hydrogens of the minor rotamer.

Table 3 ^{1}H NMR spectra of the methylene groups of **2a** in different solvents. The table lists the corresponding chemical shifts and ratio of the two rotamers: **A** (major) and **B** (minor).

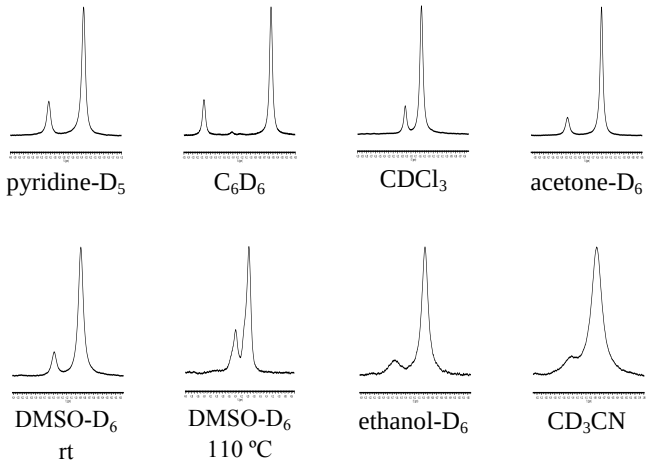

Entry	Solvent	δ_B/δ_A (ppm)	**A/B**	ε^a
1	pyridine-D_5	4.31/4.24	3.52:1	13.26
2	C_6D_6	4.21/4.05	3.65:1	2.28
3	$CDCl_3$	4.19/4.15	4.97:1	4.81
4	acetone-D_6	4.23/4.15	5.41:1	21.01
5	DMSO-D_6	4.15/4.09	5.60:1	47.24
6	DMSO-D_6	4.24/4.20[b]	3.00:1[b]	47.24
7	ethanol-D_6	4.16/4.10	6.00:1[c]	25.30
8	CD_3CN	4.14/4.09	12.00:1[c]	36.64

[a] Dielectric constant. [b] Data obtained at 110 ºC. [c] Ratio calculated from other spectrum signals.

(Fig. 4). Due to the relative spatial proximity of the β-phenyl and $H_{k'}$, the former might exert a shielding impact on the latter by polarisation and field effects.[34] The calculated dipolar

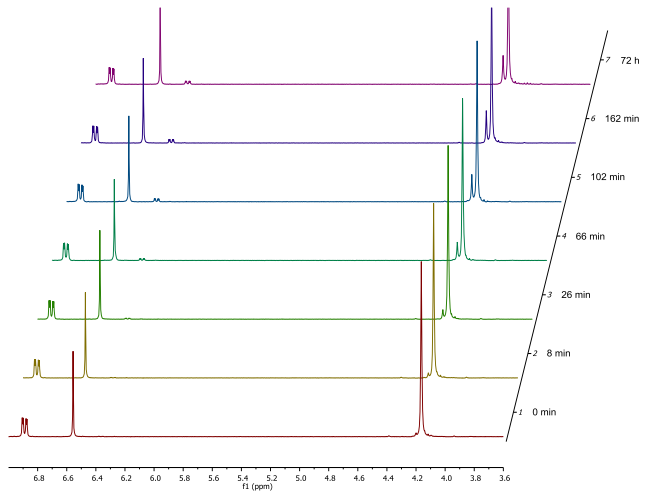

Fig. 5 In-situ ^{1}H NMR analysis of the rotamer **A** of **2a** in $CDCl_3$.

moments[35] for the rotamer **A** (3.17 D) and rotamer **B** (1.32 D) marry up with their abundance as a function of the solvent polarity; i.e., the rotamer **A** prevails in polar solvents. We managed to get a ^{1}H NMR spectrum of the pure rotamer **A** by dissolving the solid **2a** in $CDCl_3$ just before running the NMR experiment (Fig. S1). In-situ ^{1}H NMR analysis of this sample at room temperature disclosed that complete rotamer equilibration was attained after *ca.* 2 h (Figs. 5 and S2).

Rotamers were also observed for dyes of the 3-aryl-1-dibenzylamino series (Table 4, entries 1–5 and 14): the presence of electron-withdrawing groups at the *para* position of the phenyl group displaced the equilibrium towards the rotamer A (Table 4, entries 4 and 5) and vice versa (Table 4, entry 3). A quite homogeneous A/B ratio was measured for the *N*-alkylated (non-benzylic) dyes **2g–2j** (Table 4, entries 7–10). The most pronounced effect in favour of the minor rotamer B

View Article Online
DOI: 10.1039/C7GC03436A

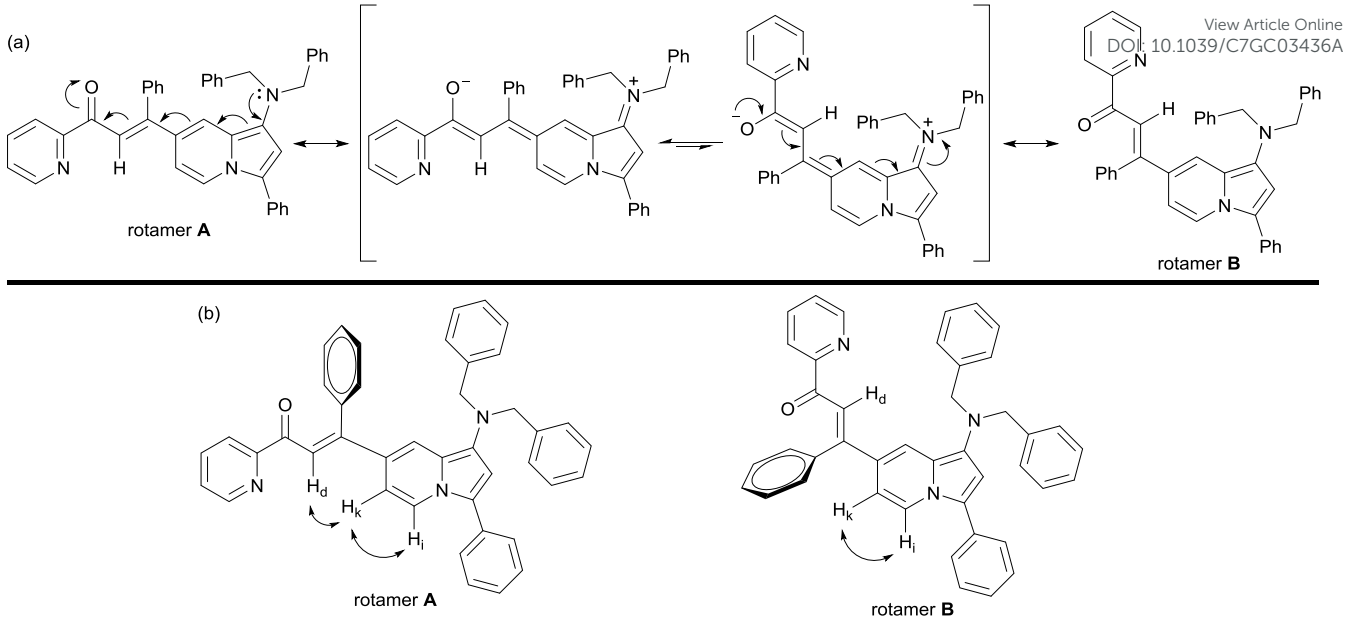

Scheme 5 (a) Proposed structures for the rotamers **A** and **B** of **2a** in solution and their resonant forms. (b) Selected NOEs.

Table 4 ^{1}H NMR chemical shifts of the dyes **2** and ratio of the two rotamers: **A** (major) and **B** (minor).

Entry	Dye	δ_B/δ_A (ppm)[a]	A/B
1	**2a**	6.86/6.35	83:17
2	**2b**	6.84/6.34	83:17
3	**2c**	6.81/6.34	78:22
4	**2d**	6.90/6.36	91:9
5	**2e**	6.95/6.38	88:12
6	**2f**	6.85[b]	>99:1
7	**2g**	6.93/6.38	83:17
8	**2h**	6.86/6.38	81:19
9	**2i**	6.84/6.33	85:15
10	**2j**	6.88/6.40	84:16
11	**2k**	6.84/6.45	70:30
12	**2l**	2.62/2.58[c]	68:32
13	**2m**	3.78/3.73[d]	79:21[d]
14	**2n**	6.97/6.41	86:14

[a] Chemical shift in $CDCl_3$ of $H_k/H_{k'}$ unless otherwise stated. [b] Only one set of signals was detected by NMR. [c] Determined from the MeAr group. [d] Determined from the OMe group.

was noted for the *N*-phenyl substituted dyes **2k** and **2l** (Table 4, entries 11 and 12), probably due to electron delocalisation of the N lone pair though the phenyl ring. This effect was of less magnitude in dye **2m** because the *p*-OMe groups work in the opposite direction (Table 4, entry 13). Startlingly, the dye **2f**, bearing two alkyl chains in the chalcone-indolizine skeleton, was held up to view as a single set of NMR signals in solution; the broad signals plotted might be linked to the existence of unresolved rotamers during the time-scale of the NMR experiment at room temperature. The larger conformational freedom of the butyl group, compared to that of the phenyl group, could account for this abnormality. As a general tendency, all the δ_B data were at higher field than the δ_A counterparts.

Mechanistic studies

The dyes **2** are trisubstituted indolizines which keep the original structure of the starting indolizine **1** and have solely reacted through the 7-position. The reactivity at this position might be supported, in part, by the deuteration studies by Engewald *et al.* to determine the exchange rate of the indolizine hydrogens in D_2O/dioxane at 50 ºC[36a] and in 0.02 M D_2SO_4/dioxane at 200 ºC.[36b] These studies established the following relative order of reactivity of the positions of the indolizine nucleus against electrophiles: 3 > 1 > > 2 > 7 ~ 5 > 6 > 8. In our case, the positions 1 and 3 are already substituted and the position 2 is more sterically encumbered than the position 7. Nevertheless, the amino group at the position 1 seems to play a paramount role in this selectivity (see below).

When the transformation of **1a** into **2a** was carried out following the standard procedure but in CD_3CO_2D instead of CH_3CO_2H, no incorporation of D was observed in **2a**; this result supports the activating character of acetic acid and rules out any structural role. In-situ NMR analysis of the reaction of **1a**

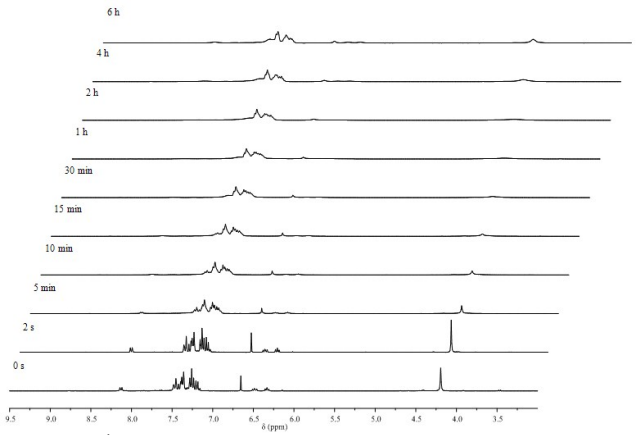

Fig. 6 In-situ ^{1}H RMN analysis of **1a** with 20 equiv. of CD_3CO_2D in $CDCl_3$.

with CD_3CO_2D in $CDCl_3$ brought forth a major depletion of the signal intensity for the indolizine hydrogen atoms (e.g., NC5-H, *ca.* 8.2 ppm) and the benzylic methylene groups (NCH_2, *ca.* 4.2 ppm) (Figs. 6 and S3). This outcome could indicate a first deuteration/protonation stage involving the nitrogen atoms. However, signals corresponding to the dye **2a** were not present in the spectra. We observed that some dye **2a** was formed after prolonged exposure of indolizine **1a** to HOAc but the reaction was much slower compared to that subjected to posterior neutralisation with sat. $NaHCO_3$, evidencing the necessity of water and/or base for the onward progress of the reaction.

On the basis of the above results, the following reaction mechanism was put forward and exemplified for the substrate **1a** (Scheme 6): two molecules of the indolizine **1a** are involved in the process, one acting as an electrophile (after proper activation) and the other one as a nucleophile. On one hand, it is our belief that **1a** possesses an enamine character and, therefore, it might experience protonation prior to hydrolysis giving the corresponding ketone, with the concomitant loss of dibenzylamine (detected in the reaction crude by GC/MS and ^{1}H NMR). On the other hand, another molecule of **1a** would act as a nucleophile through the dienamine subunit,[37] exclusively reacting at its less hindered γ position (7 position of the indolizine bicycle), by conjugate addition to an intermediate of the type **3a**. Ring opening by C–N bond cleavage in **4a** would furnish **5a** which would, eventually, undergo re-aromatisation of the indolizine core and oxidation of the dihydropyridine ring, giving rise to the dye **2a**.

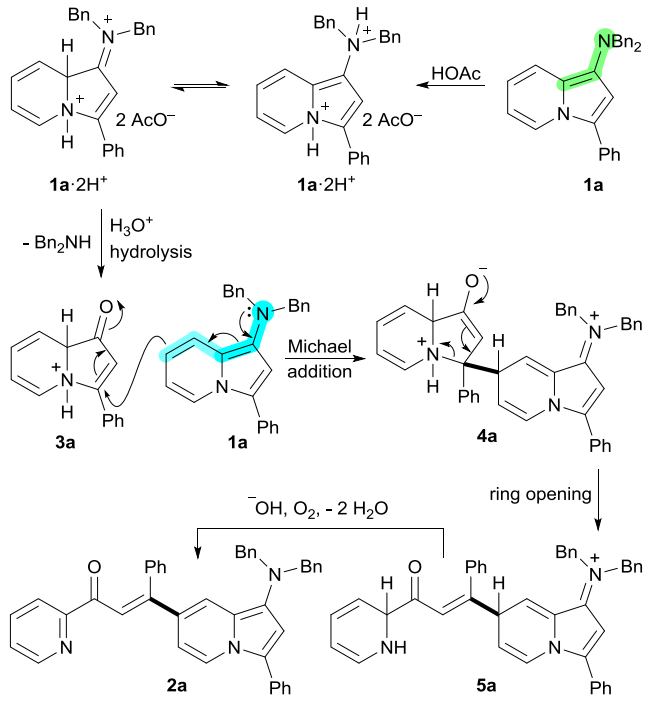

Scheme 6 Reaction mechanism proposed for the synthesis of the dye **2a**.

We got some evidence on the formation of an intermediate of the type **3a** by reacting indolizine **1a** with acetic acid, followed by acid evaporation (in air). IR analysis of a sample (Figure S4) exposed to view the absence of acetic acid [typical bands at 3500–2500 cm^{-1} (O-H); 1758 and 1714 cm^{-1} (C=O)] but the presence of a peak at 1709 cm^{-1}, typical of a five-membered α,β-unsaturated ketone [cyclopent-2-enone, 1707 cm^{-1} (C=O)]. The stretching frequency of the N-H bond in trisubstituted ammonium salts is manifested in the form of a medium-intensity wide band of pronounced structure, with the maximum interval being located at 2700-2250 cm^{-1}. We observed that type of shape in the spectrum of the sample but it is less conclusive because of its low intensity. Unfortunately, dissolution of this sample for NMR analysis mainly gave **2a** [1662 cm^{-1} (C=O)].

The amino group can be considered as both a leaving (enamine hydrolysis) and a nucleophilic group (dienamine), contributing largely to the optical and structural properties of **2** in solution. It is noteworthy the relatively good isolated yields recorded for a process which implies the reaction of a nucleophile and an in-situ generated electrophile, both derived from the same molecule. On the other hand, this process entails a change in the intrinsic electronic properties of the indolizine heterocycle because the original pyridine ring (π-deficient) acts now as a nucleophile and the pyrrole (π-exceeding) ring has been transformed into an electrophile.

Optical properties

The heterocyclic chalcone moiety, selectively grafted to the 7-position of the indolizines **2**, notably enlarges the π-conjugation system of the indolizine nucleus generating a new chromophoric assembly which confers dye attributes to them. For instance, compound **2a** in the solid state exhibits a nice reddish orange colour that resembles that of Congo Red (Fig. 7a). In acetonitrile solution (2.0×10^{-3} M), however, the pale yellow colour of the starting indolizine **1a** (λ_{max} = 340 nm) changes into reddish purple for the corresponding dye **2a** (λ_{max} = 493 nm), a colour similar to that of a young red wine (reach in anthocyanins) (Figs. 7b and S8).

Analysis of the colour of other dyes (Figs. S10, S11) could be nicely rationalised as a function of the substitution pattern. The following remarks could be made taking dye **2a** as a reference compound with λ_{max} = 493 nm: (a) the influence of the *p*-substituent in the 3-aryl-1-dibenzylamino series of dyes is scanty, with a slight bathochromic effect for those with electron-donating substituents (Table 5, compare entries 1, 4 and 5 with 2 and 3); (b) the contribution to colour of the aryl units at the β-position of the carbonyl group and 3-position of the indolizine seems to be negligible (Table 5, compare entries 6 and 14); (c) the bathochromic shift for dyes with a 1-alkylamino (non-benzylic) group is noticeable (Table 5, entries 8–10); (d) on the contrary, the 1-arylamino group leads to a hypsochromic shift with the highest ε (Table 5, entries 11 and 12); (e) the highest λ_{max} was recorded for the *N,N*-di-(4-methoxyphenyl)amino derivative **2m** (Table 5, entry 13). In summary, the chalcone-indolizine framework seems to be the chromophoric component of the dyes, whereas the amino groups are auxochromic components that modulate the colour according as the electronic character of their substituents.

Table 5 Vis radiation absorption data of the dyes **2**.[a]

Entry	Dye	λ_{max} (nm)	ε (M^{-1} cm^{-1})
1	**2a**	493	7150
2	**2b**	498	11450
3	**2c**	504	6000
4	**2d**	492	12400
5	**2e**	493	13850
6	**2f**	486	13450
7	**2g**	515	7100
8	**2h**	522	9700
9	**2i**	521	15600
10	**2j**	506	5350
11	**2k**	480	26600
12	**2l**	482	23000
13	**2m**	532	13400
14	**2n**	486	20250

[a] All the dyes were dissolved in MeCN (2.0×10^{-5} M).

A significant singularity of the dyes **2** is that their colour in the solid state varies with their particle size.[38] We briefly evaluated the influence of the particle size on the colour of **2a** by spectrophotometry and SEM (Figures S5-S7). A relatively wide maximum absorbance range of 420–520 nm was recorded for a sample of crystalline **2a**. For a mortar ground sample, a variation from reddish orange to almost black was observed (Fig. 7c); this result is consonant with the decrease in the particle size observed by SEM and the near constant absorption in all the visible spectrum.

Another remarkable attribute to be highlighted is that the dyes **2** are solvatochromic, that is, they bring into view a different colour in solution depending on the solvent utilised;[39] different sheds of pink, violet, and orange have been observed for **2a** (Table 6, Figs. 7d and S9). A correlation between the rotamer population, solvent polarity and visible absorbance can be established: the proportion of the rotamer A generally increases with the solvent polarity while the wavelength decreases ($CHCl_3$, ε = 4.81, A/B = 5.40:1, λ_{max} = 526 nm; EtOH, ε = 25.30, A/B = 6.00:1, λ_{max} = 519 nm; MeCN, ε = 36.64, A/B = 12.00:1, λ_{max} = 493 nm). This hypsochromic (blue) shift of λ_{max} while increasing the solvent polarity is a clear case of negative solvatochromism. A video on the in-situ colour change of **2a** by solvent polarity modification is available (see the ESI).

Table 6 Solvatochromic behavior of the dye **2a**.[a]

Entry	Solvent	λ_{max} (nm)	Abs	Colour
1	$CHCl_3$	526	0.352	violet
2	hexane	520	0.072	light pinkish
3	EtOH	519	0.288	violet
4	CH_2Cl_2	511	0.350	purple
5	DMF	505	0.354	red
6	dioxane	504	0.297	pinkish
7	acetone	495	0.393	orange
8	MeCN	493	0.322	orange

[a] All solutions at 2.0×10^{-5} M.

In spite of the fact that the research on functional dyes is a very active research field, its application as a practical technology is often hampered because of synthetic reasons:

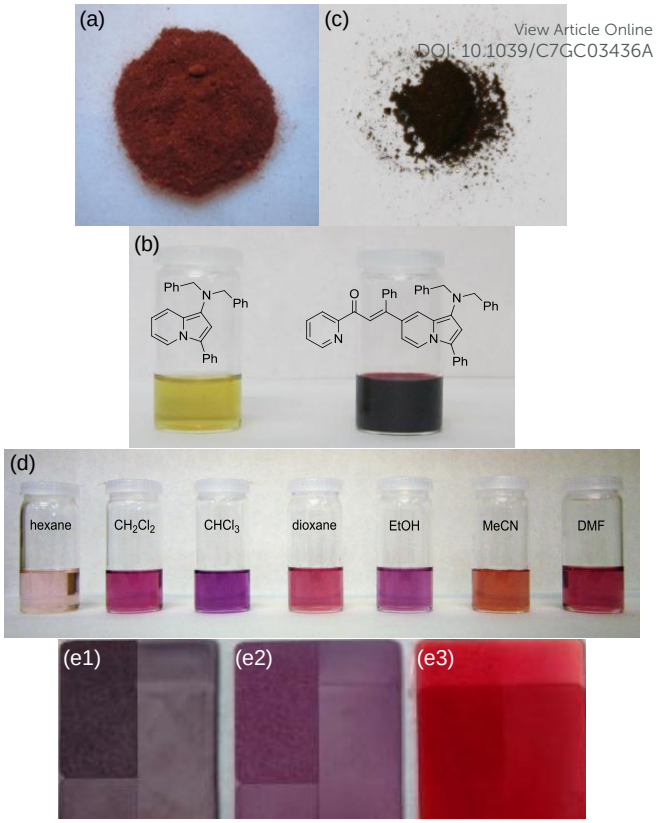

Fig. 7 The colours of the dye **2a**: (a) As obtained in the solid state. (b) The starting indolizine **1a** and the dye **2a** in acetonitrile solution (2.0×10^{-3} M). (c) **2a** after being ground in a mortar. (d) **2a** in different solvents (2.0×10^{-5} M). (e) Plates of **2a** injected into plastics: (e1) 0.2 wt% **2a** + 0.5 wt% TiO_2 in HIPS (high-impact polystyrene SB); (e2) 0.2 wt% **2a** in HIPS; (e3) 0.05 wt% **2a** in PP (polypropylene).

(a) the expensive materials and catalysts required; (b) the multi-step sequences that decrease the efficiency of the process increasing the waste; (c) the non-green conditions and reaction media used; (d) the experimental procedures are implemented at a laboratory scale but are troublesome when scaled up. We took advantage of the optical characteristics of dyes **2** to analyse their colouration power when injected into plastics. A preliminary examination revealed that migration of the dye **2a** occurred in poly(vinyl chloride) (PVC) and polyamides but high compatibility was found with polyolefins [e.g., polypropylene (PP) or polystyrene (PS)]. Three plates were prepared (Fig. 7e): two with **2a** and HIPS (high-impact polystyrene SB), with or without TiO_2, and a third one with **2a** and PP. The first conclusion is that the dye **2a** possesses a strong colouration power at a very low concentration. We were delightfully astonished to check that the solvatochromic character of the dye was also demonstrated in plastic materials transparent to the visible radiation, such as PS and PP. Indeed, three differently coloured plastic plates could be obtained with a single dye. The effect was particularly dramatic when changing the polymeric material from HIPS to PP.

Conclusions

A number of key issues have been addressed in this study. The remote-site C–H alkenylation of indolizines is feasible under metal-free conditions. The most impressive peculiarity of this transmutation is that a single starting material is deployed, with the new alkenyl substituent bound to the indolizine nucleus in the product being derived from another molecule of the starting indolizine and being incorporated through a novel regio- and stereoselective C_{sp2}–C_{sp2} bond formation. Given that the products keep the original structure with the only substitution of a hydrogen atom, the whole process could be described as a case of "molecular clone transplantation". This type of reaction in which the same compound acts as a nucleophile and electrophile with the partial grafting of the latter on the former is infrequent in organic synthesis, albeit the aldol self-condensation could be a simplistic example. These products are well-defined D-A-π-A reddish-to-deep violet dyes in the solid state which split into two rotamers in solution. An introductory study to the optical features of these dyes reveals a particle-size dependent colour, high coloration power and solvatochromic character, also in plastic materials. Moreover, the indolizine/chalcone hybrid structures obtained by this procedure are new and their properties can make improvements to current applications of indolizine- or chalcone-based materials or may allow the discovery of new applications. This survey opens a type of reactivity up to heterocyclic chemistry which might be extended to other properly substituted heterocyclic compounds. The facts that the synthetic procedure is easy (acid-base treatment), mild (ambient temperature), can be conducted in one pot from commercial chemicals and it is scalable to multigram scale pave the way for the future industrial utilisation of these materials.

Conflicts of interest

There are no conflicts to declare.

Acknowledgements

This work was generously supported by the Spanish Ministerio de Economía y Competitividad (MINECO; CTQ2011-24151 and CTQ-2015-66624-P) and the Generalitat Valenciana (GV; grants no. APOTIP/2015/014 and AEST/2015/001). M.J.A. and M.J.G.-S. are grateful to the Instituto de Síntesis Orgánica (ISO) for both pre-doctoral grants (contracts no. I-PAS-44/13 and I-PAS-11/16). We would like to acknowledge especially Dr. Diana Almasi (ISO) for optimizing the large-scale synthesis of the dye **2a** as well as IQAP Masterbatch Group S.L. and Colortech Química S.L. for testing the dyes in different plastic materials.

Notes and references

† Present address (M.J.A.): Sharda Cropchem España S. L., Carril Condomina (Atalaya Business Center), 30006 Murcia, Spain.
This article is dedicated to Prof. Irina P. Beletskaya on the occasion of her 85th birthday

1 C.-L. Sun and Z.-J. Shi, *Chem. Rev.*, 2014, **114**, 9219–9280.
2 Reviews: (*a*) B. Li and P. H. Dixneuf, *Chem. Soc. Rev.*, 2013, **42**, 5744–5767; (*b*) Y. Wu, J. Wang, F. Mao and F. Y. Kwong, *Chem. Asian J.*, 2014, **9**, 26–47; (*c*) L. Zhou and W. Lu, *Chem. Eur. J.*, 2014, **20**, 634–642; (*d*) T. Kitamura and Y. Fujiwara, in *From C-H to C-C Bonds. Cross-Dehydrogenative Coupling*, ed. C.-J. Li, The Royal Society of Chemistry, Cambridge, UK, 2015, ch. 2.
3 P. B. Arockiam and P. H. Dixneuf, *Chem. Rev.*, 2012, **112**, 5879–5918.
4 (*a*) F. W. Patureau, J. Wencel-Delord and F. Glorius, *Aldrichim. Acta*, 2012, **45**, 31–41; (*b*) B. Ye and N. Cramer, *Acc. Chem. Res.*, 2015, **48**, 1308–1318; (*c*) T. Satoh and M. Miura, in *Catalytic Transformations via C-H Activation 1*, *Science of Synthesis*, Thieme, Stuttgart, 2016, ch. 1.1.6.
5 (*a*) J. Le Bras and J. Muzart, *Chem. Rev.*, 2011, **111**, 1170–1214; (*b*) C. Huang, B. Chattopadhyay and V. Gevorgyan, *J. Am. Chem. Soc.*, 2011, **133**, 12406–12409; (*c*) P. K. Doman and V. M. Dong, in *Catalytic Transformations via C-H Activation 1*, *Science of Synthesis*, Thieme, Stuttgart, 2016, ch. 1.1.5.
6 (*a*) D. Leow, G. Li, T.-S. Mei and J.-Q. Yu, *Nature*, 2012, **486**, 518–522; (*b*) Y. Deng and J.-Q. Yu, *Angew. Chem. Int. Ed.*, 2015, **54**, 888–891; (*c*) M. Bera, A. Maji, S. K. Sahoo and D. Maiti, *Angew. Chem. Int. Ed.*, 2015, **54**, 8515–8519; (*d*) Z. Zhang, K. Tanaka and J.-Q. Yu, *Nature*, 2017, **543**, 538–542.
7 Y. Nakao, in *Catalytic Transformations via C-H Activation 1, Science of Synthesis*, Thieme, Stuttgart, 2016, ch. 1.2.
8 P. Wen, Y. Li, K. Zhou, C. Ma, X. Lan, C. Ma and G. Huang, *Adv. Synth. Catal.*, 2012, **354**, 2135–2140.
9 (*a*) L.-Q. Zhang, S. Yang, X. Huang, J. You and F. Song, *Chem. Commun.* **2013**, *49*, 8830–8832; (*b*) X.-F. Yang, X.-H. Hu, C. Feng and T.-P. Loh, *Chem. Commun.*, 2015, **51**, 2532–2535; (*c*) P. Kannaboina, K. A. Kumar and P. Das, *Org. Lett.*, 2016, **18**, 900–903; (*d*) B. J. Gorsline, L. Wang, P. Ren and B. P. Carrow, *J. Am. Chem. Soc.*, 2017, **139**, 9605‑9614.
10 (*a*) Y. Huang, F. Song, Z. Wang, P. Xi, N. Wu, Z. Wang, J. Lan and J. You, *Chem. Commun.*, 2012, **48**, 2864–2866; (*b*) Y.-Y. Yu and G. I. Georg, *Chem. Commun.*, 2013, **49**, 3694–3696.
11 (*a*) J. Koubachi, S. Berteina-Raboin, A. Mouaddib and G. Guillaumet, *Synthesis*, 2009, 271–276; (*b*) H. Zhan, L. Zhao, N. Li, L. Chen, J. Liu, J. Liao and H. Cao, *RSC Adv.*, 2014, **4**, 32013–32016.
12 H. Hu, Y. Liu, H. Zhong, Y. Zhu, C. Wang and M. Ji, *Chem. Asian J.*, 2012, **7**, 884–888.
13 (*a*) H. E. Eastman, C. Jamieson and A. J. B. Watson, *Aldrichim. Acta*, 2015, **48**, 51–55; (*b*) D. Prat, A. Wells, J. Hayler, H. Sneddon, R. McElroy, S. Abou-Shehadad and P. J. Dunne, *Green Chem.*, 2016, **18**, 288–296.
14 Review: Y. Segawa, T. Maekawa and K. Itami, *Angew. Chem. Int. Ed.*, 2015, **54**, 66–81.
15 Selected reviews: (*a*) Y. Zhou and J. Yoon, *Chem. Soc. Rev.*, 2012, **41**, 52–67; (*b*) H. S. Jung, X. Chen, J. S. Kim and J. Yoon, *Chem. Soc. Rev.*, 2013, **42**, 6019–6031; (*c*) A. N. Uglov, A. Bessmertnykh-Lemeune, R. Guillard, A. D. Averin and I. P. Beletskaya, *Russ. Chem. Rev.*, **2014**, *83*, 196–224.
16 Reviews: (*a*) Y. Ooyama and Y. Harima, *Eur. J. Org. Chem.*, 2009, 2903–2934; (*b*) Y. Wu and W. Zhu, *Chem. Soc. Rev.*, 2013, **42**, 2039–2058; (*c*) Viewpoint: L. Kloo, *Chem. Commun.*, 2013, **49**, 6580–6583.
17 Reviews: (*a*) V. R. Vemula, S. Vurukonda and C. K. Bairi, *Int. J. Pharm. Sci. Rev. Res.*, 2011, **11**, 159–163; (*b*) G. S. Sing and E. E. Mmatli, *Eur. J. Med. Chem.*, 2011, **46**, 5237–5257.
18 Reviews: (*a*) B. Urmila, *J. Pharm. Res. (Mohali, India)*, 2012, **5**, 4236–4241; (*b*) S. N. A. Bukhari, M. Jasamai and I. Jantan, *Mini Rev. Med. Chem.*, 2012, **12**, 1394–1403; (*c*) H. Prashar, A. Chawla, A. K. Sharma and R. Kharb, *Int. J. Pharm. Sci. Res.*, 2012, **3**, 1913–1927; (*d*) J. Handzlik, A. Matys and K. Kieć-

Knonowicz, *Antibiotics*, 2013, **2**, 28–45. (*e*) P. Singh, A. Anand and V. Kumar, *Eur. J. Med. Chem.*, 2014, **85**, 758–777.

19 See, for instance: (*a*) T.-D. Tran, T.-T.-N. Nguyen, T.-H. Do, T.-N.-P. Huynh, C.-D. Tran and K.-M. Thai, *Molecules*, 2012, **17**, 6684–6696; (*b*) C. G. D. Raj, B. K. Sarojini, S. Hegde, S. Sreenivasa, Y. S. Ravikumar, V. Bhanuprakash, Y. Revanaiah and R. Ragavendra, *Med. Chem. Res.*, 2013, **22**, 2079–2087; (*c*) P. Sharma, S. Karma, F. Ali, S. Anthal, V. K. Gupta, I. A. Khan, S. Singh, P. L. Sangwan, K. A. Suri, B. D. Gupta, D. K. Gupta, P. Dutt, R. A. Vishwakarma and N. K. Satti, *Med. Chem. Res.*, 2013, **22**, 3969–3983.

20 S. M. Bronner, G.-Y. J. Im and N. K. Garg, in *Heterocycles in Natural Product Synthesis*, ed. K. C. Majumdar and S. K. Chattopadhyay, Wiley-VCH, Weinheim, 2011, pp. 221–265.

21 G. Desimoni, G. Faita and P. Quadrelli, *Chem. Rev.*, 2014, **114**, 6081–6129.

22 (*a*) G. L. Fletcher Jr., S. L. Bender and D. H. Wadsworth (Eastman Kodak Co.), Eur. Pat. 68876A1, 1983; *Chem. Abstr.*, 1984, **100**, 122772; (*b*) Y. Inagaki, K. Adachi and M. Yabe (Fuji Photo Film Co., Ltd.), Jap. Pat. 02062280A, 1990; *Chem. Abstr.*, 1991, **114**, 52945; (*c*) A. Takazawa and T. Kobayashi, (Fuji Photo Film Co., Ltd.), Jap. Pat. 03113847A, 1991; *Chem. Abstr.*, 1991, **115**, 267063; (*d*) T. Suzuki, M. Shinkai and N. Nanba (TDK Electronics Co., Ltd.), Jap. Pat. 07126543A, 1995; *Chem. Abstr.*, 1995, **123**, 183678.

23 Y.-S. Jung and J.-Y. Jaung, *Dyes Pigments*, 2005, **65**, 205–209.

24 Y. Inagaki and T. Kubo (Fuji Photo Film Co., Ltd.), Jap. Pat. 03074471A, 1991; *Chem. Abstr.*, 1991, **115**, 138212.

25 J. Tanabe, M. Shinkai, M. Tsuchiya (TDK Electronics Co., Ltd.), Jap. Pat. 2008101064A, 2008; *Chem. Abstr.*, 2008, **148**, 520703.

26 (*a*) A. Rotaru, I. Druta, E. Avram and R. Danac, *ARKIVOC*, 2009, **xiii**, 287–299; (*b*) M. F. Z. J. Amaral, L. A. Deliberto, C. R. de Souza, R. M. Z. G. Naal, Z. Naal and G. C. Clososki, *Tetrahedron*, 2014, **70**, 3249–3252; (*c*) E. Kim, Y. Lee, S. Lee and S. B. Park, *Acc. Chem. Res.*, 2015, **48**, 538−547; (*d*) Y. R. Song, C. V. Limb and T. W. Kima, *Luminescence*, 2016, **31**, 364‑371; (*e*) Y. Zhang, J. Garcia-Amorós, B. Captain and F. M. Raymo, *J. Mater. Chem. C*, 2016, **4**, 2744–2747; (*f*) V. K. Outlaw, J. Zhou, A. E. Bragg and C. A. Townsend, *RSC Adv.*, 2016, **6**, 61249–61253.

27 (*a*) K. Rurack, J. L. Bricks, G. Reck, R. Radeglia and U. Resch-Genger, *J. Phys. Chem. A*, 2000, **104**, 3087–3109; (*b*) S. H. Mashraqui, T. Khan, S. Sundaram and S. Ghadigaonkar, *Tetrahedron Lett.*, 2008, **49**, 3739–3743; (*c*) S. A. El-Daly, M. Gaber, S. S. Al-Shihry and Y. S. El Sayed, *J. Photochem. Photobiol. A: Chem.*, 2008, **195**, 89–98; (*d*) M. Gaber, S. A. El-Daly and Y. S. Y. El-Sayed, *J. Mol. Struct.*, 2009, **922**, 51–57; (*e*) Y. S. El-Sayed, *Opt. Laser Technol.*, 2013, **45**, 89–95; (*f*) Y. S. El-Sayed and M. Gaber, *Spectrochim. Acta, Part A,* 2015, **137**, 423–431; (*g*) Y. Shinozaki, T. Arai, *Heterocycles*, 2017, **95**, 972–979.

28 See, for instance: F. Alonso, Y. Moglie, G. Radivoy, M. Yus, *J. Org. Chem.*, 2013, **78**, 5031–5037.

29 (*a*) M. J. Albaladejo, F. Alonso and M. Yus, *Chem. Eur. J.*, 2013, **19**, 5242–5245; (*b*) M. J. Albaladejo, F. Alonso and M. J. González-Soria, *ACS Catal.*, 2015, **5**, 3446–3456.

30 M. J. Albaladejo, M. J. González-Soria and F. Alonso, *J. Org. Chem.*, 2016, **81**, 9707–9717.

31 F. Alonso and M. J. Albaladejo, (Universidad de Alicante), PCT-ES2014/070921, 2014.

32 CCDC-995503 (**2a**) and CCDC-995504 (**2c**) contain the supplementary crystallographic data for this paper. These data can be obtained free of charge from The Cambridge Crystallographic Data Centre via www.ccdc.cam.ac.uk/data_request/cif
Selected X-ray crystallographic data for 2a: $C_{42}H_{33}N_3O$, *M* = 595.71, triclinic, space group P–1, orange needles, *a* = 10.823(6), *b* = 12.460(7), *c* = 13.441(8) Å, *T* = 298(1), *Z* = 2, 13758 reflections measured, 5777 unique (R_{int} = 0.2677), $wR(F^2)$ = 0.2533.
Selected X-ray crystallographic data for 2c: $C_{44}H_{37}N_3O_3$, *M* = 655.77, triclinic, space group P–1, orange plates, *a* = 12.1335(16), *b* = 12.3113(16), *c* = 12.6442(17) Å, *T* = 297(2), *Z* = 2, 15271 reflections measured, 6260 unique (R_{int} = 0.0744), $wR(F^2)$ = 0.1668.

33 J. L. Chiara and A. Gómez-Sánchez, in *The Chemistry of Enamines*, ed. Z. Rappoport, Wiley, Chichester, UK, 1994, ch. 5.

34 C. W. Anson and D. M. Thamattoor, *J. Org. Chem.*, 2012, **77**, 1693–1700.

35 The dipolar moments were determined by calculation with the PM3 semiempirical method: J. J. P. Stewart, *J. Comput. Chem.*, 1991, **12**, 320–341.

36 (*a*) W. Engewald, M. Mühlstädt and C. Weiss, *Tetrahedron*, 1971, **27**, 4171–4178; (*b*) W. Engewald, M. Mühlstädt and C. Weiss, *Tetrahedron*, 1971, **27**, 851–864.

37 P. W. Hickmott, in *The Chemistry of Enamines*, ed. Z. Rappoport, Wiley, Chichester, UK, 1994, ch. 26.

38 A. M. Gueli, G. Bonfiglio, S. Pasquale and S. O. Troja, *Color Res. Appl.*, 2016, **42**, 236–243.

39 C. Reichardt, *Chem. Rev.*, 1994, **94**, 2319–2358.

View Article Online
DOI: 10.1039/C7GC03436A

Table of contents entry

The metal-free regio- and diastereoselective remote C-H self-alkenylation of indolizines leads to a new family of solvatochromic dyes.